15TH IEA HEAT PUMP CONFERENCE
MAY 26–29, 2026 | HOFBURG
VIENNA 2026
DECARBONISATION THROUGH INNOVATION

Performance evaluation of a direct expansion air-solar-ground CO_2 heat pump for water heating applications

Marco Tancon[a], Mohammad Mozafarivanani[a], Riccardo Conte[a], Emanuele Zanetti[b], Marco Azzolin[a*]

[a]Department of Industrial Engineering, University of Padova, Via Venezia 1, 35131 Padova, Italy
[b]Department of Process and Energy, Delft University of Technology, Leeghwaterstraat 39, 2628 CB Delft, the Netherlands

Abstract

The transition toward efficient and low-carbon heating technologies is a key requirement for sustainable development, with heat pumps playing a central role in residential applications. However, conventional heat pumps face intrinsic limitations: air-source units suffer from seasonal temperature fluctuations, ground-source units ensure stable performance but face high installation costs, and solar-assisted systems are constrained by irradiation availability. Hybrid heat pumps that combine multiple renewable sources offer a potential solution to mitigate these drawbacks and enhance overall system performance.
This study develops a numerical model of an innovative direct-expansion multisource CO_2 heat pump equipped with dedicated evaporators to utilize air, solar, and ground energy. Solar input is extracted from photovoltaic-thermal (PV-T) collectors, ground energy from borehole heat exchangers (BHEs), and air energy from a finned-coil heat exchanger. The prototype can operate in two configurations, solar-air and ground-air modes, in which CO_2 evaporates simultaneously in two heat exchangers: flooded operation in the solar or ground evaporator and dry expansion in the air evaporator.
Simulations investigate the effects of air temperature, soil temperature, solar irradiance on system performance. The coefficient of performance (COP) shows strong sensitivity to environmental conditions, increasing by approximately 5.3% per 1 K rise in air temperature in both operating modes. In solar-air mode, COP increases by 3% per 100 W/m² of global tilted irradiance, whereas ground-air operation exhibits a 1.1% COP gain per 1 K rise in soil temperature. Compared to a reference air-source heat pump, the multisource configuration achieves a 6-15% improvement, depending on renewable energy availability. Performance can be further enhanced by increasing the number of BHEs or PV-T panels. In ground-air mode, using one to three BHEs leads to 8-21% COP increase, while in solar-air mode, deploying one to four PV-T collectors improves COP by 4-22%.

Keywords: Carbon dioxide; Multisource heat pump; Solar energy; Geothermal energy; Direct expansion; Simultaneus operations;

1. Introduction

Heat pumps are considered a fundamental technology for decarbonizing space heating and domestic hot water production as well as supporting on-site renewable energy usage. Most heat pumps rely on a single low-temperature source, such as air-source heat pumps (ASHPs), ground-source heat pumps (GSHPs), and solar-source heat pumps (SSHPs). ASHPs are widely used in buildings and are highly influenced by external temperature fluctuations; their efficiency declines as the air temperature decreases, especially when the heating demand is higher. GSHPs can offer a higher energy efficiency than ASHPs, but the drawback is related to their higher installation costs due to the drilling of the borehole. SSHPs integrating photovoltaic and thermal (PV-T) collectors can enhance seasonal performance compared to ASHPs; however, they are penalized by solar

* Corresponding author. *E-mail address:* marco.azzolin@unipd.it

radiation availability [1]. Both GSHP and SSHP systems can operate in two configurations: direct expansion (DX), where the refrigerant evaporates as it flows directly through boreholes or solar collectors, and indirect expansion, where a secondary fluid absorbs heat from boreholes or collectors and transfers it to the refrigerant through a heat exchanger [2].

To overcome the limitations related to the use of a single-energy source, hybrid heat pump systems that exploit two or more low-temperature sources simultaneously can be a solution. However, even if the adoption of natural refrigerants has become increasingly important in recent years due to evolving regulations such as the European Union's F-gas Regulation (EU) 2024/573 [3], most heat pump systems studied in the literature use synthetic refrigerants and data on systems using natural refrigerants are scarce. Two examples are: Sazon et al. [4] who analyzed an IDX solar-assisted ground-source CO_2 heat pump using solar collectors and borehole heat exchangers (BHEs) as evaporators, and Pelella et al. [5] who optimized a three-source heat pump utilizing air, solar, and ground working with propane as refrigerant, showing a potential efficiency gain (on the COP) from 3.4 to 11.8 based on location and investment.

The present paper numerically investigates a hybrid multi-source direct-expansion heat pump, integrating three energy sources: air, solar, and ground. The system utilizes a finned coil heat exchanger for the air source, PV-T collectors for the solar source, and a U-tube BHE for the ground source. The finned coil evaporator is fed in dry expansion, while the PV-Ts and BHE operate in flooded mode, overcoming possible maldistribution issues of the refrigerant mass flow rate. Carbon dioxide is used as the refrigerant. The hybrid system operates in two configurations, each simultaneously exploiting two energy sources: solar-air mode or ground-air mode, where PV-T collectors or BHEs run simultaneously with the finned coil heat exchanger. The hybrid system behaves as a DX dual-source heat pump in each mode. Notably, this configuration differs from existing series and parallel setups. A comprehensive numerical model of the hybrid heat pump system has been developed in MATLAB® to compare the performance of the ground-air and solar-air modes against conventional ASHPs. This model enables a systematic analysis of the performance of this novel multisource heat pump under varying thermal loads and environmental conditions.

2. Layout of the system

Fig. 1 shows the layout of the direct-expansion multisource heat pump system (Fig. 1a) and the logarithmic pressure-enthalpy diagram representing the thermodynamic cycle at design conditions (Fig. 1b). The heat pump, which works with CO_2 as refrigerant, can exploit three renewable heat sources: air, solar, and ground. The main components of the system include a compressor (COMP), a gas cooler (GC), an internal heat exchanger (IHE), an electronic expansion valve (EEV), which regulates high pressure, and a low-pressure receiver (REC). The heat pump is equipped with three evaporators to exploit different thermal sources: a finned coil heat exchanger (FCHE), three PV-T collectors (tilted at 45°), and a U-tube borehole heat exchanger. Two operating modes are analyzed: solar-air mode (SA-mode), where the finned coil and PV-T evaporators run simultaneously, and ground-air mode (GA-mode), where the FCHE and BHE operate together. The schematic of the SA-mode is taken from a real heat pump installation, studied experimentally and numerically in a previous work.

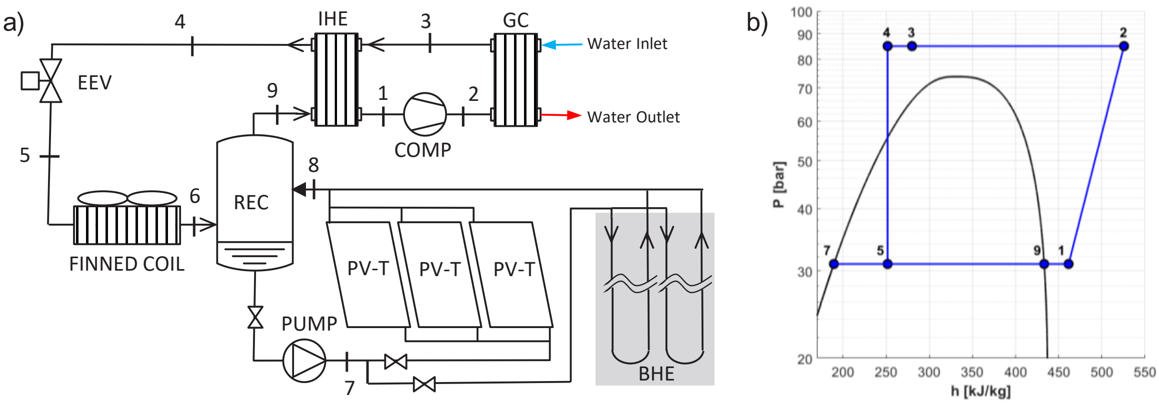

Figure 1. a) Layout of the hybrid heat pump system. b) Thermodynamic cycle at the design condition plotted in a log(p)-h diagram.

As shown in Fig. 1, the superheated refrigerant (point 1) is compressed and sent to the gas cooler for cooling (point 2). It then moves through the internal heat exchanger, undergoing additional subcooling (point 3). After expanding in the EEV, it enters the two-phase region and evaporates inside the finned coil heat exchanger (point 5). With increased vapor quality, the CO_2 flows into the low-pressure receiver, where the liquid and vapor phases separate. At point 7, the liquid CO_2 from the bottom of the REC is directed either to the BHE (in GA-mode) or to the PV-T collectors (in SA-mode). After partial evaporation, the refrigerant returns to the receiver. Finally, the saturated vapor (point 9) is first superheated in the IHE before returning to the compressor. Points 6 (outlet of the finned coil evaporator) and 8 (outlet of the solar or ground evaporators) are between points 5 and 9 in the thermodynamic cycle, as partial evaporation occurs in these heat exchangers.

This configuration allows the FCHE and either the PV-T collectors or BHEs to operate simultaneously. Importantly, the FCHE, PV-T collectors, or BHE, and the REC share the same pressure level. Therefore, the receiver regulates low pressure by conservation of mass and energy balances within the CO_2 system, while acting as a liquid-vapor separator. In this way, only vapor is directed toward the compressor, whereas liquid is supplied to the PV-T or BHE evaporators.

3. Numerical modeling

This section presents the heat pump model, implemented in MATLAB®. The model is used to assess performance and energy flows under various environmental conditions and operating modes. It simulates the supercritical CO_2 cycle, determining the thermodynamic states of the refrigerant. Thermodynamic properties of CO_2, water, and air are obtained using Refprop 10.0 [6]. The model assumes negligible thermal losses and pressure drops within the heat exchangers and compressor, and considers the throttling process to be isenthalpic.

The compressor is modelled based on three polynomial equations and their corresponding coefficients reported in [7] with inputs of evaporating temperature, high pressure, and compressor speed. For GC, IHE, FCHE, and PV-T collectors, a distributed parameter approach is used. In these models, the energy, momentum, and continuity equations are solved sequentially within each discretized section.

Since the variation of CO_2 properties is high in the GC, the model tracks temperature and enthalpy changes along its length in each discretized element. The model takes as input the mass flow rates and inlet conditions of both the refrigerant and water and provides the outlet temperatures and the heating capacity. Fluid flow is assumed to be equally distributed across channels, and heat transfer is calculated iteratively using the logarithmic mean temperature difference method. The same procedure is considered for the IHE. Both models were validated against experimental data in [7] and in [8], respectively.

The FCHE model divides the total volume into identical elements that are analysed in sequence along the refrigerant flow path. For each segment, the refrigerant outlet conditions are determined using the effectiveness-NTU method. This model is described in detail and validated against the experimental data in [9]. The model of PV-T collectors that is validated against experimental data in [10] considers the thermal capacities of the glass cover, PV cell, and absorber plate. Heat losses to the environment are assumed to occur exclusively through the top and bottom surfaces of the collector, with the edges being perfectly insulated. The system of partial differential equations, derived from the application of conservation laws, is solved by assuming constant fluid properties, such as density, enthalpy, and pressure, within each spatial and temporal discretization. Additionally, heat transfer coefficients (HTCs), void fraction, and pressure drops are calculated using established correlations found in the literature. It is worth mentioning that the model accounts for the cooling effect of refrigerant evaporation on cell temperature and thus on the electric production of the PV cells. Using this model, simulations performed with and without the refrigerant cooling effect were compared, showing that PV power production increased by approximately 8% when the cooling effect was included.

The REC is modelled having the refrigerant mass flow rate, evaporator outlet enthalpy and temperature, refrigerant conditions at the throttling valve outlet, and the liquid level height inside the tank as inputs. The model calculates the temporal variation of the liquid level and the evaporation temperature/pressure and estimates the mass flow rate circulating in the loop, which differs from that sucked by the compressor based on the mass and energy conservation in the REC and corresponding pressure losses of the refrigerant returning from the evaporators. This model has been validated in [10].

In the present work, the heat pump model developed in [8] is updated integrating the newly developed direct-expansion BHE model, in which refrigerant flows directly. The refrigerant is modelled in terms of enthalpy change along the circuit and integrated with the rest of the system geometry using a quasi-3D thermal resistance and capacity model. This method accounts for heat transfer within the fluid (i.e., CO_2) mainly through convection, and from the surrounding materials (grout and soil) through conduction. The model used is based on an approach developed by Bauer et al. [11] and is applied to a single U-loop borehole heat exchanger. Heat transfer behaviour changes depending on whether the CO_2 is in a single-phase or two-phase state, with different methods used to estimate the HTC in each case. For two-phase CO_2 inside pipes, the correlation developed by Cheng et al. [12] is used, while the HTC for single-phase flow is evaluated according to the Gnielinski [13] equation. Regarding the thermal capacities, the capacity of the soil has been neglected, but the heat capacity of the grout is included. The governing equation for the enthalpy changes of the fluid within the circuit during time is derived from the energy balance of an infinitesimal element of the fluid in the BHE. The results of the present model have been validated against the experimental data of Badache et al. [14], finding a 4.1% average error in the prediction of the evaporating capacity inside the BHE.

The solution algorithm starts with the definition of first attempt values of the evaporation temperature and superheating at the compressor suction. The COMP submodel calculates the refrigerant mass flow rate and the discharge enthalpy. Then the submodel of the GC provides the refrigerant enthalpy at the outlet and the water mass flow rate. Subsequently, the IHE submodel calculates a new value of superheating at the compressor inlet and enthalpy at the inlet of the EEV. Finally, the evaporator submodels (FCHE + PV-T or BHE) provide an updated value of the evaporation temperature. The cycle restarts from the COMP model and repeats until convergence values of the evaporation temperature and superheating are obtained.

The model outputs are the thermodynamic properties of the refrigerant along the refrigerant loop, the overall power consumption (P_{tot}), which accounts for fan, circulation pump and compressor power consumptions, the heating capacity (Q_{HP}), and the COP of the heat pump defined as:

$$\mathrm{COP} = \frac{Q_{HP}}{P_{tot}} \tag{1}$$

4. Design of the multisource heat pump

To design the length and the number of BHEs, some preliminary simulations have been conducted considering Padova as the reference location: annual average air and soil temperatures of 7 °C and 13 °C, respectively, and average monthly solar irradiance on the horizontal plane equal to 300 W/m^2. The chosen operating conditions for SA-mode e GA-mode are: water temperature lift from 30 °C to 40 °C at the GC, maximum compressor speed, fan speed equal to 50%, high-pressure equal to 85 bar. The PV-T characteristics of the SA-mode and the BHE characteristics of the GA-mode are listed in Table 1, with only the length of the BHE as the independent variable. Both configurations share an identical air evaporator, which consists of a finned coil heat exchanger comprising four copper tube circuits (10.12 mm outer diameter, 0.35 mm wall thickness) arranged in four rows and 22 columns, with a row spacing of 21.65 mm and a tube spacing of 25 mm, thickness of the aluminum fins equal to 0.12 mm and 3.2 mm spacing. The outcomes of the design procedure indicated that, at the design condition, one BHE with a borehole depth equal to 35 m results in the same evaporating and heating capacity as compared to the SA-mode. In particular, the air-mode has an evaporating capacity of 3.16 kW, while SA-mode achieves 3.45 kW, and GA-mode reaches 3.5 kW. The PV-T and BHE evaporators have evaporating capacities that are 53% and 56% lower, respectively, compared to the finned coil heat exchanger. In fact, these evaporators are designed to work simultaneously with the air evaporator, not to replace it. This design allows installation even in locations with limited ground or roof availability and also enables retrofitting existing air-source heat pumps to enhance their efficiency.

Table 1. Design conditions and component characteristics.

Design conditions	Details
Location	Padova, North Italy
Average monthly solar irradiance	300 W/m² on the horizontal plane
Annual average soil temperature	13 °C
Annual average air temperature	7 °C
PV-T collectors (SA-mode)	270 W nominal power output, 1.64 m² surface area of each PV-T collectors, multicrystalline silicon Plate-and-tube heat exchanger with 15 copper tubes (serpentine configuration), 8 mm OD, and 1 mm plate thickness
BHE (GA-mode)	Borehole radius 39 mm, tube external diameter 7.2 mm, tube internal diameter mm 5.6, distance between the two axes of the two tubes of U tube 23 mm
FCHE	Four copper tube circuits (10.12 mm outer diameter, 0.35 mm wall thickness) arranged in four rows and 22 columns

5. Results and discussion

In this section, the model of the multi-source heat pump is used to compare the steady-state performance of the hybrid heat pump system in SA-mode and GA-mode. As shown in Section 3, the BHE evaporator is sized to deliver the same evaporating capacity as the PV-T evaporator under the designed operating conditions. The analysis examines the effect of water temperature demand, environmental conditions, and the number of PV-T collectors and BHEs on system performance. In this context, the coefficient of performance is for the comparison and the total electricity consumed by the heat pump system includes power used by the compressor, the fan of the finned coil evaporator, and the pumps for both the PV-T and BHE evaporators.

5.1. Effect of environmental conditions

The results of the investigation of the effects of air temperature (T_{air}), solar irradiance (GTI) and soil temperature (T_{soil}) on the performance of the multisource heat pump operating in both SA-mode and GA-mode are reported in Fig. 2 and Fig. 3. In particular, the COP maps obtained for the SA-mode are reported as a function of air temperature and GTI, while those for the GA-mode are reported as a function of air and soil temperatures. The results refer to varying T_{air} between 0 °C and 16 °C, T_{soil} from 7 °C to 15 °C, and GTI between 300 W/m² and 1100 W/m², with compressor speed fixed at 100%, fan speed at 50%, high pressure at 85 bar, and gas cooler water temperature increase from 20 °C to 50 °C. Fig. 3 shows the evaporating temperature under the same operating conditions as in Fig. 2.

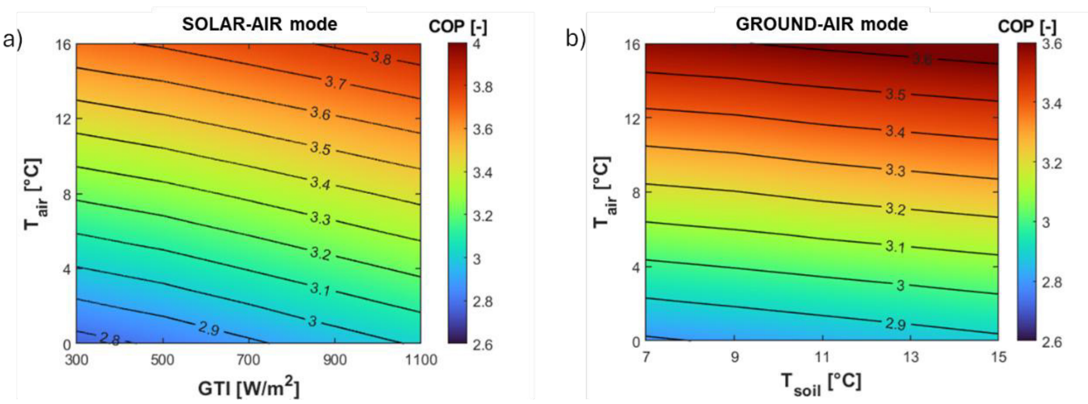

Figure 2. Iso-COP maps of the multisource heat pump as a function of (a) air temperature (T_{air}) and solar irradiance (GTI) for the SA-mode and (b) air temperature and soil temperature (T_{soil}) for the GA-mode.

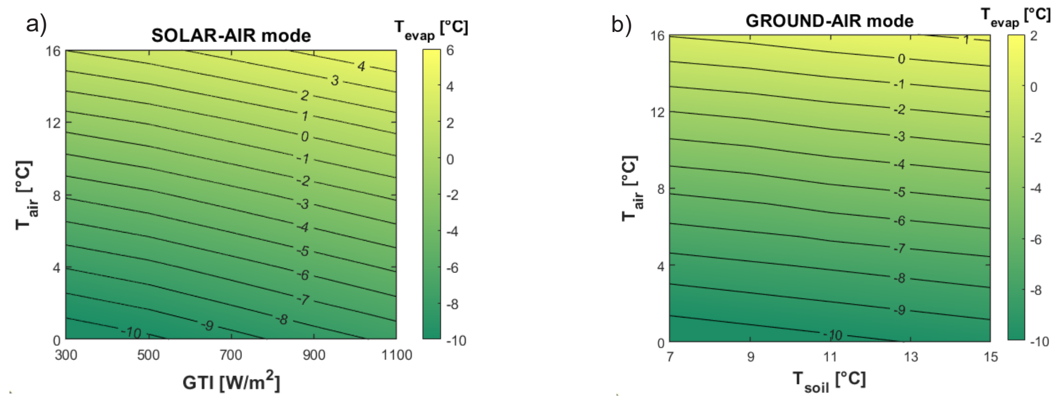

Figure 3. Iso-T_{evap} maps of the multisource heat pump as a function of (a) air temperature (T_{air}) and solar irradiance (GTI) for the SA-mode and (b) air temperature and soil temperature (T_{soil}) for the GA-mode.

In SA-mode, COP rises from 2.7 to 3.8 as T_{air} increases from 0 °C to 16 °C and GTI from 300 W/m^2 to 1100 W/m^2. The results suggest that the influence of T_{air} is stronger, with a 5.6% COP increase per 1 K rise in T_{air} compared to 3% COP increase per 100 W/m^2 rise in GTI. This behaviour is due to the evaporating capacity of the PV-T collectors being 53% lower than that of the finned-coil heat exchanger under design conditions.

Similarly, in GA-mode, COP ranges from 2.6 to 3.8, mainly driven by T_{air} rather than T_{soil}. COP rises by 5.1% per 1 K increase of T_{air}, while T_{soil} contributes about 1.1% per 1 K. The weaker effect of T_{soil} is explained by the BHE evaporating capacity being 56% lower than that of the finned coil heat exchanger at the design point. Fig. 3 shows that T_{evap} ranges from 5 °C to -10 °C as T_{air} increases from 0 °C to 16 °C and GTI from 300 W/m^2 to 1100 W/m^2 (Fig. 3a) in SA-mode and from 1 °C to -10 °C in GA-mode as T_{air} is between 0 °C and 16 °C, and T_{soil} is ranging from 7 °C to 15 °C, (Fig. 3b). A clear dependence on air temperature can be observed, whereas the effect of solar irradiance and soil temperature is weaker. This behaviour is consistent with the relative evaporating capacities of the heat exchangers, with the finned-coil evaporator providing the dominant contribution.

5.2. Effect of heating demand characteristics

In this section, the system performance is studied under varying heating demands at the gas cooler, and the results are compared with those obtained in air-mode operation. Simulations were conducted for two applications, keeping other conditions constant: space heating (SH) with a water supply temperature from 30 °C to 40 °C, and domestic hot water (DHW) production with a supply temperature from 20°C to 50 °C. To evaluate the performance of the multisource heat pump in SA-mode and GA-mode against the air-mode (where the heat pump operates solely with the air source), the following operating conditions are set: T_{air} of 8 °C, fan speed at 50%, compressor running at 100%, high pressure at 85 bar, and refrigerant mass flow rate inside the PV-T or BHE evaporators equal to half of the mass flow rate processed by the compressor.

Figure 4 presents COP for SH and DHW under two opposite environmental scenarios: low contributions of solar and ground sources (T_{soil} = 7 °C, GTI = 300 W/m^2) in Fig. 3a, and high contributions of solar and ground sources (T_{soil} = 15 °C, GTI = 1100 W/m^2) in Fig. 3b. With low contributions of energy sources (Fig. 3a), SA-mode and GA-mode perform approximately similarly for both applications, achieving COP values of 3.13 for SH and 3.35 for DHW. Both operating modes outperform the air-mode by approximately 6.5%. Under higher solar and ground contributions (Figure 4b), the COP improves: the GA-mode reaches COP values of 3.37 for SH and 3.42 for DHW, while the SA-mode exhibits the same COP for SH and 5% higher values for DHW production compared to GA-mode. The COP for both operating modes surpasses the air-mode performance by 14.5% for SH application. For DHW, the COP in SA-mode is 14.1% higher compared to air-mode, while the improvement in GA-mode is only 9.2%.

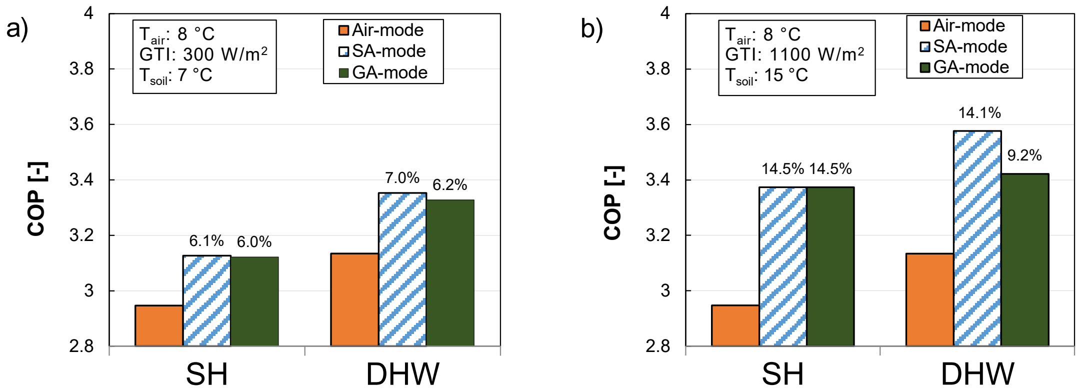

Figure 4. Comparison between COP achieved in air-mode, SA-mode and GA-mode for space heating (SH) and domestic hot water (DHW) applications. a) T_{air} = 8 °C, GTI = 300 W/m^2, T_{soil} = 7 °C; b) T_{air} = 8 °C, GTI = 1100 W/m^2, T_{soil} = 15 °C.

5.3. Effect of the number of BHEs and PV-T collectors

The numerical model of the multisource heat pump is used here to study the effect of varying number of BHEs (from 1 to 3) in GA-mode and PV-T collectors (from 1 to 4) in SA-mode on the system performance. Adjusting the number of PV-T collectors or BHEs changes the total evaporation surface area, which significantly impacts the overall evaporation process. Simulations were carried out at two levels of solar irradiance (GTI: 300 W/m^2 and 1100 W/m^2) and soil temperatures (T_{soil}: 7 °C and 13 °C), with all other conditions kept constant: compressor speed at 100%, fan speed at 50%, high pressure at 85 bar, water heated from 30 °C to 40 °C, refrigerant mass flow rate through the solar or geothermal evaporators set to half of the compressor's flow rate, and T_{air} of 4 °C.

The impact of the number of PV-T collectors (SA-mode) and BHEs (GA-mode) on COP and heat extracted at the gas cooler (Q_{GC}) is shown in Tables 2 and 3, respectively. In GA-mode, increasing the number of BHEs improves COP and Q_{GC} for both values of T_{soil}. When the number of BHEs increases from 1 to 3, the COP improves from 2.81 to 3.01 at a soil temperature of 7 °C (representing a 7% increase), and from 2.86 to 3.17 at T_{soil} = 13 °C (marking an 11% COP increase). A similar pattern can be observed in the heat delivered at the gas cooler, which rises from 4460 W to 4780 W at T_{soil} = 7 °C and from 4550 W to 5000 W at T_{soil} = 13 °C. In SA-mode, the effect of adding more PV-T collectors is beneficial for both COP and Q_{GC}, regardless of the irradiance level. Specifically, increasing the number of PV-T collectors from 1 to 4 at a GTI of 300 W/m^2 boosts the COP from 2.69 to 2.85 (a 6% increase), while at 1100 W/m^2 it increases from 2.77 to 3.15 (a 14% improvement). Correspondingly, Q_{GC} rises from 4230 W to 4510 W at 300 W/m^2 and from 4370 W to 4940 W at 1100 W/m^2.

It is interesting to note that both operating modes outperform air-mode, even when just one PV-T collector or BHE is installed. Overall, GA-mode sees an 8 – 21% COP gain over air-mode, while SA-mode achieves a 4 – 22% increase. These results highlight the system’s flexibility, delivering enhanced performance even when considering a limited PV-T evaporator area or a single shallow BHE. These results also highlight the trade-off between evaporator sizing and system performance, as increasing the PV-T or BHE area leads to progressively smaller performance gains.

Table 2. COP and Q_{GC} values for the SA-mode and GA-mode when T_{air} = 4°C: effect of the number of PV-T collectors in SA-mode for two GTI values (300 and 1100 W/m^2); effect of the number of BHEs in GA-mode for two T_{soil} values (7°C and 13°C).

	COP [-]		**Q_{GC} [W]**	
GTI [W/m^2]	**300**	**1100**	**300**	**1100**
Air Mode	2.62		4110	
N_{PVT} = 1	2.68	2.77	4230	4370
N_{PVT} = 2	2.75	2.89	4340	4570
N_{PVT} = 3	2.80	3.01	4430	4810
N_{PVT} = 4	2.85	3.15	4510	4930

Table 3. COP and Q_{GC} values for the SA-mode and GA-mode when T_{air} = 4°C: effect of the number of PV-T collectors in SA-mode for two GTI values (300 and 1100 W/m^2); effect of the number of BHEs in GA-mode for two T_{soil} values (7°C and 13°C).

	COP [-]		**Q_{GC} [W]**	
T_{soil} [°C]	**7**	**13**	**7**	**13**
Air Mode	2.62		4110	
N_{BHE} = 1	2.81	2.86	4460	4550
N_{BHE} = 2	2.92	3.04	4640	4820
N_{BHE} = 3	3.01	3.17	4780	5010

6. Conclusions

This study presents a numerical analysis of a multisource CO_2 heat pump prototype capable of operating in two configurations: solar-air (SA-mode) and ground-air (GA-mode), using air, solar, and ground as low-temperature heat sources. In both modes, CO_2 evaporates simultaneously in two heat exchangers through direct expansion. The borehole heat exchanger model was developed using a quasi-3D thermal resistance–capacity approach and validated against literature data.

The performance of the multisource heat pump is assessed under varying thermal loads and environmental conditions, and compared with those of a reference air-source heat pump. The results revealed that the COP increases with rising air temperature in both operating modes, by 5.6% per 1 K in SA-mode and 5.1% in GA-mode. Additionally, SA-mode benefits from higher solar irradiance, with a 3% COP gain per 100 W/m² of global tilted irradiance, while GA-mode shows a 1.1% COP increase per 1 K rise in soil temperature. Water temperatures at the gas cooler also influence the COP, with domestic hot water production generally yielding higher COP values than space heating. Overall, the multisource heat pump outperforms the air-mode configuration, with efficiency improvements ranging from 6.5% under low solar or geothermal energy input up to 14.5% when both sources are at high contribution. System performance further improves by increasing the number of BHEs or PV-T collectors. In GA-mode, using one to three BHEs leads to an 8 – 21% COP improvement, while in SA-mode, deploying one to four PV-T collectors increases COP by 4 – 22% compared to using only air as the low-temperature heat source.

A comprehensive cost-benefit or life-cycle economic analysis, which would require site-specific installation costs and market-dependent price data, represents a relevant direction for future work. In addition, the model provides a useful tool for evaluating control strategies aimed at maximizing key system performance indicators.

References

[1] Poppi S, Sommerfeldt N, Bales C, Madani H, Lundqvist P. Techno-economic review of solar heat pump systems for residential heating applications. *Renewable and Sustainable Energy Reviews* 2018; **81**:22–32.

[2] Kamel R S, Fung A S, Dash P R H. Solar systems and their integration with heat pumps: A review. *Energy Build* 2015; **87**:395–412.

[3] EU No 2024/573 Regulation (EU) 2024/573 of the European Parliament and of the Council of 7 February 2024 on fluorinated greenhouse gases, amending Directive (EU) 2019/1937 and repealing Regulation (EU) No 517/2014.

[4] Sazon T A, Zhang Q, Nikpey H. Comparison of different configurations of a solar-assisted ground-source CO2 heat pump system for space and water heating using Taguchi-Grey Relational analysis. *Energy Convers Manag* 2024; **300**

[5] Pelella F, Zsembinzki G, Viscito L, William Mauro A, Cabeza L F. Thermo-economic optimization of a multi-source (air/sun/ground) residential heat pump with a water/PCM thermal storage. *Appl Energy* 2023; **331**.

[6] Lemmon E W, Huber M L, McLinden M O. NIST standard reference database 23: Reference fluid thermodynamic and transport properties-REFPROP (version 9), *NIST* 2010.

[7] Zanetti E, Bordignon S, Conte R, Bisi A, Azzolin M, Zarrella A. Experimental and numerical analysis of a CO2 dual-source heat pump with PVT evaporators for residential heating applications. *Appl Therm Eng* 2023; **233**.

[8] Conte R, Zanetti E, Tancon M, Azzolin M, Girotto S, Del Col D. The advantage of running a direct expansion CO2 heat pump with solar-and-air simultaneous heat sources: experimental and numerical investigation. *Appl Energy* 2024; **369**.

[9] Zanetti E, Bonduà S, Bortolin S, Bortolotti V, Azzolin M, Tinti F. Sequential coupled numerical simulations of an air/ground-source heat pump: Validation of the model and results of yearly simulations. *Energy Build* 2022; **277**.

[10] Zanetti E, Azzolin M, Conte R, Girotto S, Del Col D. Experiments and dynamic modelling of dry expansion and flooded evaporators in a CO2 solar assisted heat pump. *Appl Therm Eng* 2022; **217**.

[11] Bauer D, Heidemann W, Diersch H-J G. Transient 3D analysis of borehole heat exchanger modelling. *Geothermics* 2011; **40**:250–60

[12] Cheng L, Ribatski G, Thome J R. New prediction methods for CO2 evaporation inside tubes: Part II - An updated general flow boiling heat transfer model based on flow patterns. *Int J Heat Mass Transf* 2008; **51**:125–35.

[13] Gnielinski V. New equations for heat and mass transfer in turbulent pipe and channel flow. *International chemical engineering* 1976; **16**:359–67.

[14] Badache M, Ouzzane M, Eslami-Nejad P, Aidoun Z. Experimental study of a carbon dioxide direct-expansion ground source heat pump (CO2-DX-GSHP). *Appl Therm Eng* 2018; **130**:1480–8